World Academy of Science, Engineering and Technology
International Journal of Mathematical and Computational Sciences
Vol:4, No:10, 2010

A Cell-centered Diffusion Finite Volume Scheme and it's Application to Magnetic Flux Compression Generators

Qiang ZHAO, Yina SHI, Guangwei YUAN, and Zhiwei DONG

Open Science Index, Mathematical and Computational Sciences Vol:4, No:10, 2010 publications.waset.org/5135.pdf

Abstract—A cell-centered finite volume scheme for discretizing diffusion operators on distorted quadrilateral meshes has recently been designed and added to APMFCG to enable that code to be used as a tool for studying explosive magnetic flux compression generators. This paper describes this scheme. Comparisons with analytic results for 2-D test cases are presented, as well as 2-D results from a test of a "realistic" generator configuration.

Keywords—cell-centered FVM, distorted meshes, diffusion scheme, MFCG.

I. Introduction

INVESTIGATING the numerical schemes with high accuracy for diffusion equation on distorted meshes is very important in Lagrangian hydrodynamics and magnetohydrodynamics. Lagrangian method is widely used for the reason that it has a simple structure and keeps clear track of the material interface. Since the computational mesh in Lagrangian method is embedded in the fluid, it will follow the movement of the fluid and consequently, even being orthogonal initially, will become highly skewed or highly distorted, which will reduce the accuracy of the corresponding discrete schemes or even worse, stop the whole computation. If the discrete schemes have a high adaptability to the Lagrangian mesh, then the number of the mesh reconstruction will be much reduced or even better, the whole computation will proceed without any mesh reconstruction.

Magnetic flux compression generators (MFCGs) power supplies provide compact inexpensive generators of high current (megamperes), high energy (megajoules), and short current risetime (microseconds). Applications of these generators in plasma, solid-state, particle, and optical physics research have been reviewed by Knoepfel [1] and Fowler [2].

Helically-wound generators, described by Shearer, et al. [3] and Crawford and Damerow [4], have the advantage of a high initial inductance, permitting a potentially high amplification factor. Figure 1 shows a sketch of a typical generator. An initial pulsed current in the outer helical coil winding establishes magnetic flux between the coil and the inner metallic cylinder, referred to as the armature. The armature contains high explosive, which is detonated from one end, driving the armature towards the coil at high velocity. The inductance decrease in the helical winding is a result both of the decrease in radial separation between the armature and the coil and of the decrease in coil axial length as the armature short circuits successive turns of the coil. This decrease in inductance, combined with the coil's tendency to conserve flux, leads to amplification of the electrical current which can be delivered to an external load. Chemical energy stored in the explosive is converted to kinetic energy of the armature. This energy in turn is transformed by the coil magnetic field into electrical energy delivered to the external load.

A two-dimensional magnetohydrodynamics (MHD) code which can be used to study at least isolated sections of the generator geometry has been constructed. The basic approach to be taken is to add a magnetic field solver, Joule heating, self-consistent magnetic forces, and an external circuit equation to the 2-D material response code.

This paper describes a cell-centered diffusion finite volume scheme. a two-dimensional finite difference magnetic field solver has been developed using the scheme to treat the flux compression and the nonlinear temperature-dependent resistive diffusion into both conductors.

Authors are with Institute of Applied Physics and Computational Mathematics, Beijing, 100088, P.R.China. e-mail: Q.ZHAO.CN@gmail.com.

This project is supported by the Foundation of National Key Laboratory of Computational Physics and National Natural Science Foundation of China(No.10902017).

II. Cell-centered diffusion finite volume scheme

A. Problem and notations

Let Ω be an open bounded polygonal subset of R^2 with boundary $\partial\Omega$ and $u = u(x)$ the solution of the following steady diffusion problem:

$$-\nabla \cdot (\lambda \nabla u) = f, \quad \text{in } \Omega \tag{1}$$

where u is homogeneous to a temperature, λ is a scalar diffusion coefficient, and f denotes a source term.

The domain Ω is paved with a collection of non-overlapping convex quadrangles: $\{\text{K,L,}\dots\}$ and with each cell K we associate one point (the so-called collocation point or cell-centered) denoted also by K: the barycenters is a qualified candidate but other points can be chosen. Denote the cell vertex by $A, B, \dots$, and the cell side by σ. If the cell side σ is a common edge of cells K and L, and its vertices are A and B, then we denote $\sigma = K|L = BA$ and its length is denoted by $|A - B|$.

Let $\mathcal{J}$ be the set of all cells, $\mathcal{E}$ be the set of all cell side, and $\mathcal{E}_K$ be the set of all cell side of cell K. Denote $\mathcal{E}_{int} = \mathcal{E} \cap \Omega$, $\mathcal{E}^0_{int} = \{\sigma \in \mathcal{E}_{int} : \sigma \cap \partial\Omega = \emptyset\}$, $\mathcal{E}_{ext} = \mathcal{E} \cap \partial\Omega$. Denote $h = \left(\sup_{K\in\mathcal{J}} m(K)\right)^{1/2}$, where $m(K)$ is the area of cell K. The distance from the cell-center K (resp. L) to the edge σ is

Open Science Index, Mathematical and Computational Sciences Vol:4, No:10, 2010 publications.waset.org/5135.pdf

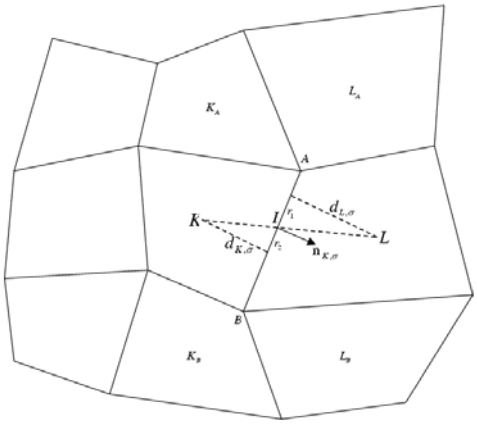

Fig. 1. Stencil and notation.

denoted by $d_{K,\sigma}$(resp. $d_{L,\sigma}$),see Figure 1. I denotes a point on the line AB which is usually the intersection point of line segment KL with σ or the midpoint of the edge σ.

We adopt the following notations (see Fig.1). $\vec{n}_{K,\sigma}$(resp. $\vec{n}_{L,\sigma}$) is the outward unit vector normal to the edge σ of cell K (resp. L). There holds $\vec{n}_{K,\sigma} = -\vec{n}_{L,\sigma}$ for $\sigma = K|L$. $\vec{t}_{K,\sigma}$ denotes the unit vector tangential to σ, see Figure 2.

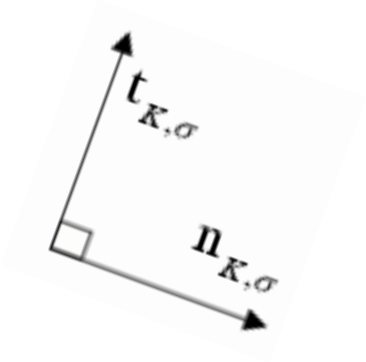

Fig. 2. Outward unit vector normal to σ and unit vector tangent to σ.

B. Construction of the scheme

By integrating (1) over the cell K, and using Green formula, one obtains

$$\sum_{\sigma\in\mathcal{E}_K} \mathcal{F}_{K,\sigma} = \int_K f(x)dx, \tag{2}$$

where the continuous diffusion flux on edge σ is

$$\mathcal{F}_{K,\sigma} = -\int_\sigma \lambda(x)\nabla u(x)\cdot\vec{n}_{K,\sigma}dl. \tag{3}$$

Note that

$$\begin{aligned} L-I &= I\vec{L} = d_{L,\sigma}\vec{n}_{K,\sigma} + r_1\vec{t}_{K,\sigma},\\ A-B &= B\vec{A} = |A-B|\vec{t}_{K,\sigma},\\ I-K &= K\vec{I} = d_{K,\sigma}\vec{n}_{K,\sigma} + r_2\vec{t}_{K,\sigma}, \end{aligned} \tag{4}$$

where

$$r_1 = \frac{(L-I, A-B)}{|A-B|}, r_2 = \frac{(I-K, A-B)}{|A-B|}. \tag{5}$$

It is straightforward to express the outward unit vector normal to σ using the third equation of (4) and the expression $I-K = K\vec{I} = |I-K|\vec{t}_{KI}$, where $\vec{t}_{KI}$ is the unit vector tangential to $I-K$: $\vec{n}_{K,\sigma} = \frac{1}{\cos\theta_{K,\sigma}}\vec{t}_{KI} - \tan\theta_{K,\sigma}\vec{t}_{K,\sigma}$, where $\theta_{K,\sigma}$ denotes the angle between $\vec{n}_{K,\sigma}$ and $I-K$.

The continuous diffusion flux can be written as

$$\begin{aligned} \mathcal{F} =& \tan\theta_{K,\sigma}\int_\sigma \lambda(x)\nabla u(x)\cdot\vec{t}_{K,\sigma}dl\\ &- \frac{1}{\cos\theta_{K,\sigma}}\int_\sigma \lambda(x)\nabla u(x)\cdot\vec{t}_{KI}dl. \end{aligned} \tag{6}$$

In order to discretize the above continuous diffusion flux, we use the Taylor expansion for the function u, and then obtain

$$\begin{aligned} u(I)-u(K) &= \nabla u(x)\cdot(I-K) + \int_0^1 (H_I - H_K)sds,\\ u(A)-u(B) &= \nabla u(x)\cdot(A-B) + \int_0^1 (H_A - H_B)sds, \end{aligned} \tag{7}$$

where $H_K = \big(\nabla^2 u(sx+(1-s)K)(K-x), K-x\big)$, $\nabla^2 u(sx+(1-s)K)$ denotes the Hessian matrix of u at the point $sx+(1-s)K$. The notations H_I, H_A and H_B have the similar meaning.

Note that $I-K = K\vec{I} = |I-K|\vec{t}_{KI}$ and $A-B = B\vec{A} = |A-B|\vec{t}_{K,\sigma}$. By multiplying the above two equations by $\lambda(x)$ and integrating on the edge σ, one obtains

$$\begin{aligned} \int_\sigma \lambda(x)(u(I)-u(K))dl =& \int_\sigma \lambda(x)\nabla u(x)|I-K|\cdot\vec{t}_{KI}dl\\ &+ \int_\sigma \left(\lambda(x)\int_0^1 (H_I-H_K)sds\right)dl,\\ \int_\sigma \lambda(x)(u(A)-u(B))dl =& \int_\sigma \lambda(x)\nabla u(x)|A-B|\cdot\vec{t}_{K,\sigma}dl\\ &+ \int_\sigma \left(\lambda(x)\int_0^1 (H_A-H_B)sds\right)dl. \end{aligned} \tag{8}$$

So we have

$$\begin{aligned} \int_\sigma \lambda(x)\nabla u(x)\cdot\vec{t}_{KI}dl =& \frac{|A-B|}{|I-K|}\lambda_{K,\sigma}(u(I)-u(K))\\ &- \frac{1}{|I-K|}\int_\sigma \left(\lambda(x)\int_0^1 (H_I-H_K)sds\right)dl, \end{aligned} \tag{9}$$

and similarly

$$\begin{aligned} \int_\sigma \lambda(x)\nabla u(x)\cdot\vec{t}_{K,\sigma}dl =& \lambda_{K,\sigma}(u(A)-u(B))\\ &- \frac{1}{|A-B|}\int_\sigma \left(\lambda(x)\int_0^1 (H_A-H_B)sds\right)dl, \end{aligned} \tag{10}$$

where $\lambda_{K,\sigma} = \frac{1}{|A-B|}\int_\sigma \lambda(x)dl$ is the average value of $\lambda(x)$ along σ in the cell K. The second terms of right hand side in the above two equations are $O(h^2)$. Substitute (9) and (10)

Open Science Index, Mathematical and Computational Sciences Vol:4, No:10, 2010 publications.waset.org/5135.pdf

into (6) to obtain

$$\begin{aligned}\mathcal{F}_{K,\sigma} &= \tan\theta_{K,\sigma}\left[\lambda_{K,\sigma}(u(A)-u(B))\right.\\ &\quad \left.-\frac{1}{|A-B|}\int_\sigma\left(\lambda(x)\int_0^1(H_A-H_B)sds\right)dl\right]\\ &\quad -\frac{1}{\cos\theta_{K,\sigma}}\left[\frac{|A-B|}{|I-K|}\lambda_{K,\sigma}(u(I)-u(K))\right.\\ &\quad \left.-\frac{1}{|I-K|}\int_\sigma\left(\lambda(x)\int_0^1(H_I-H_K)sds\right)dl\right]\\ &= -\tau_{K,\sigma}\left[u(I)-u(K)-D_{K,\sigma}(u(A)-u(B))\right]\\ &\quad + R_{K,\sigma}\end{aligned} \tag{11}$$

where

$$\begin{aligned}&\tau_{K,\sigma}=\frac{|A-B|\lambda_{K,\sigma}}{|I-K|\cos\theta_{K,\sigma}}=\frac{|A-B|\lambda_{K,\sigma}}{d_{K,\sigma}},\\ &D_{K,\sigma}=\frac{\sin\theta_{K,\sigma}|I-K|}{|A-B|}=\frac{r_2}{|A-B|},\\ &R_{K,\sigma}=\int_\sigma\int_0^1\frac{\lambda(x)}{d_{K,\sigma}}\left[H_I-H_K-D_{K,\sigma}(H_A-H_B)\right]sdsdl\\ &=O(h^2).\end{aligned} \tag{12}$$

Similarly, we have

$$\begin{aligned}\mathcal{F} &= -tau_{L,\sigma}\left[u(I)-u(L)-D_{L,\sigma}(u(B)-u(A))\right]\\ &\quad + R_{L,\sigma},\end{aligned} \tag{13}$$

where

$$\begin{aligned}&\tau_{L,\sigma}=\frac{|A-B|\lambda_{L,\sigma}}{d_{L,\sigma}}, D_{L,\sigma}=\frac{r_1}{|A-B|},\\ &R_{L,\sigma}=\int_\sigma\int_0^1\frac{\lambda(x)}{d_{L,\sigma}}\left[H_I-H_L-D_{L,\sigma}(H_B-H_A)\right]sdsdl\\ &=O(h^2).\end{aligned} \tag{14}$$

From the continuity of the normal flux

$$\mathcal{F}_{K,\sigma}=-\mathcal{F}_{L,\sigma} \tag{15}$$

we get

$$\begin{aligned}u(I) &= \frac{1}{\tau_{K,\sigma}+\tau_{L,\sigma}}\left[\tau_{K,\sigma}u(K)+\tau_{L,\sigma}u(L)\right.\\ &\quad \left.+(\tau_{K,\sigma}D_{K,\sigma}-\tau_{L,\sigma}D_{L,\sigma})(u(A)-u(B))\right]\\ &\quad +\frac{1}{\tau_{K,\sigma}+\tau_{L,\sigma}}(R_{K,\sigma}+R_{L,\sigma}).\end{aligned} \tag{16}$$

Substitute (16) into (11) to obtain

$$\begin{aligned}\mathcal{F}_{K,\sigma} &= -\tau_\sigma\left[u(L)-u(K)-D_\sigma(u(A)-u(B))\right]\\ &\quad +\tilde{R}_{K,\sigma},\end{aligned} \tag{17}$$

where

$$\begin{aligned}&\tau_\sigma=\frac{\tau_{K,\sigma}\tau_{L,\sigma}}{\tau_{K,\sigma}+\tau_{L,\sigma}}, D_\sigma=D_{K,\sigma}+D_{L,\sigma}=\frac{(L-K,A-B)}{|A-B|^2},\\ &\tilde{R}_{K,\sigma}=\frac{\tau_{L,\sigma}R_{K,\sigma}-\tau_{K,\sigma}R_{L,\sigma}}{\tau_{K,\sigma}+\tau_{L,\sigma}}.\end{aligned} \tag{18}$$

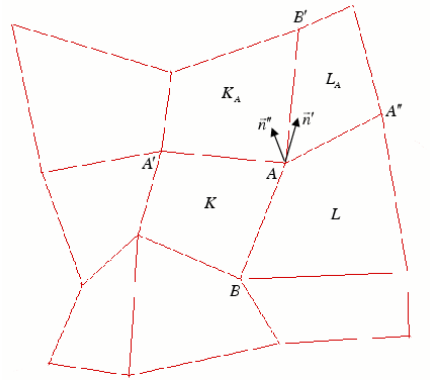

Fig. 3. Stencil of cell vertex.

Similarly, we have

$$\begin{aligned}\mathcal{F}_{L,\sigma} &= -\tau_\sigma\left[u(K)-u(L)-D_\sigma(u(B)-u(A))\right]\\ &\quad +\tilde{R}_{L,\sigma},\end{aligned} \tag{19}$$

where

$$\tilde{R}_{K,\sigma}=\frac{\tau_{K,\sigma}R_{L,\sigma}-\tau_{L,\sigma}R_{K,\sigma}}{\tau_{K,\sigma}+\tau_{L,\sigma}}. \tag{20}$$

Obviously there holds

$$\tilde{R}_{K,\sigma}=-\tilde{R}_{L,\sigma} \tag{21}$$

Let $\mathbf{F}_{K,\sigma}$ be the discrete normal flux on edge $\sigma=K|L=BA$ of cell K defined as follows:

$$\mathbf{F}_{K,\sigma}=\begin{cases}-\tau_\sigma\left[u_L-u_K-D_\sigma(u_A-u_B)\right],\forall\sigma\in\mathcal{E}_{int}^0,\\ -\tau_\sigma\left[u_L-u_K-D_\sigma u_A\right],\forall\sigma\in\mathcal{E}_{int},B\in\partial\Omega,\\ -\tau_\sigma\left[u_L-u_K+D_\sigma u_B\right],\forall\sigma\in\mathcal{E}_{int},A\in\partial\Omega,\\ \tau_{K,\sigma}u_K,\forall\sigma\in\mathcal{E}_{ext}.\end{cases} \tag{22}$$

With the definition of $\mathbf{F}_{K,\sigma}$, the finite volume scheme is constructed as follows:

$$\sum_{\sigma\in\mathcal{E}_K}\mathbf{F}_{K,\sigma}=f_K m(K),\quad \forall K\in\mathcal{J}. \tag{23}$$

It is obvious that there are the vertex unknowns in addition to cell-centered unknowns in the expression (17) and (19) of flux. Now we consider how to eliminate the vertex unknowns locally, or approximate the vertex unknowns by the neighboring cell-centered unknowns. Suppose that zigzag line segment $A'AA''$ lies on the discontinuous line (see Fig.3), line segments BA and AB' are not discontinuous line. $\vec{n}'$ (resp. $\vec{n}''$) denotes unit vector normal to $A'A$ (resp. AA'') (upward direction).

Let $\lambda|_K(A)$ denote the limit of λ on cell K to vertex A. $\lambda|_{K_A}(A)$, $\lambda|_{L_A}(A)$ and $\lambda|_L(A)$ have the similar definition. So we have $\lambda|_{K_A}(A)=\lambda|_{L_A}(A)$, $\lambda|_K(A)=\lambda|_L(A)$.

Let $\frac{\partial u}{\partial\vec{n}'}|_K(A)$ denote the limit of $\frac{\partial u}{\partial\vec{n}'}$ on cell K to vertex A. $\frac{\partial u}{\partial\vec{n}'}|_{K_A}(A)$, $\frac{\partial u}{\partial\vec{n}''}|_{L_A}(A)$, and $\frac{\partial u}{\partial\vec{n}''}|_L(A)$ have the similar definition, where $\frac{\partial u}{\partial\vec{n}'}=\nabla u\cdot\vec{n}'$ and $\frac{\partial u}{\partial\vec{n}''}=\nabla u\cdot\vec{n}''$.

Suppose the following condition is fulfilled:

$$\begin{aligned}&\lambda|_{K_A}(A)\frac{\partial u}{\partial\vec{n}'}|_{K_A}(A)+\lambda|_{L_A}(A)\frac{\partial u}{\partial\vec{n}''}|_{L_A}(A)\\ =&\lambda|_K(A)\frac{\partial u}{\partial\vec{n}'}|_K(A)+\lambda|_L(A)\frac{\partial u}{\partial\vec{n}''}|_L(A)\end{aligned} \tag{24}$$

Open Science Index, Mathematical and Computational Sciences Vol:4, No:10, 2010 publications.waset.org/5135.pdf

Let $\Omega = \Omega_1 \bigcup \Gamma \bigcup \Omega_2$, $\bar{\Omega}_1 \bigcap \bar{\Omega}_2 = \Gamma$, where Γ is the discontinuous line.

Now we distinguish two cases.

Case 1. K_A, A and L_A are collinear or K, A and L are collinear.

Firstly, assume K, A and L are collinear. There is

$$\lambda|_K(A)\frac{\partial u}{\partial \vec{KA}}|_K(A) = \lambda|_L(A)\frac{\partial u}{\partial \vec{AL}}|_L(A), \tag{25}$$

where $\vec{KA}$ denotes the unit vector tangent to KA and $\vec{AL}$ denotes the unit vector tangent to AL. Note that

$$\begin{aligned} &\lambda|_K(A) = \lambda|_L(A), \lambda(K) - \lambda(L) = O(h),\\ &\frac{\partial u}{\partial \vec{KA}}|_K(A) = \frac{u(A)-u(K)}{|A-K|} + O(h),\\ &\frac{\partial u}{\partial \vec{AL}}|_L(A) = \frac{u(L)-u(A)}{|L-A|} + O(h). \end{aligned} \tag{26}$$

Suppose

$$\lambda(K)\frac{u_A - u_K}{|A-K|} = \lambda(L)\frac{u_L - u_A}{|L-A|}. \tag{27}$$

A simple calculation shows

$$u_A = \frac{1}{\frac{\lambda(K)}{|A-K|} + \frac{\lambda(L)}{|L-A|}}\left[\frac{\lambda(K)}{|A-K|}u_K + \frac{\lambda(L)}{|L-A|}u_L\right]. \tag{28}$$

Similarly, when K_A, A and L_A are collinear, we set

$$u_A = \frac{1}{\frac{\lambda(K_A)}{|A-K_A|} + \frac{\lambda(L_A)}{|L_A-A|}}\left[\frac{\lambda(K_A)}{|A-K_A|}u_{K_A} + \frac{\lambda(L_A)}{|L_A-A|}u_{L_A}\right]. \tag{29}$$

Case 2. K_A, A and L_A are not collinear, and K, A and L are not collinear.

Let $\vec{n} = \vec{n}' + \vec{n}''$. Then there exists α_1, α_2, β_1 and β_2, such that

$$\vec{n} = \alpha_1 A\vec{K}_A + \alpha_2 A\vec{L}_A = \beta_1 \vec{KA} + \beta_2 \vec{LA}. \tag{30}$$

Let $\vec{t}$ denotes the unit vector normal to $\vec{n}$. The dot products of (30) with $\vec{n}$ and $\vec{t}$, respectively, give

$$\begin{aligned} &|\vec{n}|^2 = \alpha_1 A\vec{K}_A\cdot\vec{n} + \alpha_2 A\vec{L}_A\cdot\vec{n}, 0 = \alpha_1 A\vec{K}_A\cdot\vec{t} + \alpha_2 A\vec{L}_A\cdot\vec{t};\\ &|\vec{n}|^2 = \beta_1 \vec{KA}\cdot\vec{n} + \beta_2 \vec{LA}\cdot\vec{n}, 0 = \beta_1 \vec{KA}\cdot\vec{t} + \beta_2 \vec{LA}\cdot\vec{t}. \end{aligned} \tag{31}$$

One obtains the expression of α_1, α_2, β_1 and β_2:

$$\begin{aligned} &\alpha_1 = \frac{|\vec{n}|^2 A\vec{L}_A\cdot\vec{t}}{\begin{vmatrix} A\vec{K}_A\cdot\vec{n} & A\vec{L}_A\cdot\vec{n} \\ A\vec{K}_A\cdot\vec{t} & A\vec{L}_A\cdot\vec{t}\end{vmatrix}}, \alpha_2 = -\frac{|\vec{n}|^2 A\vec{K}_A\cdot\vec{t}}{\begin{vmatrix} A\vec{K}_A\cdot\vec{n} & A\vec{L}_A\cdot\vec{n} \\ A\vec{K}_A\cdot\vec{t} & A\vec{L}_A\cdot\vec{t}\end{vmatrix}},\\ &\beta_1 = \frac{|\vec{n}|^2 \vec{LA}\cdot\vec{t}}{\begin{vmatrix} \vec{KA}\cdot\vec{n} & \vec{LA}\cdot\vec{n} \\ \vec{KA}\cdot\vec{t} & \vec{LA}\cdot\vec{t}\end{vmatrix}}, \beta_2 = -\frac{|\vec{n}|^2 \vec{KA}\cdot\vec{t}}{\begin{vmatrix} \vec{KA}\cdot\vec{n} & \vec{LA}\cdot\vec{n} \\ \vec{KA}\cdot\vec{t} & \vec{LA}\cdot\vec{t}\end{vmatrix}}. \end{aligned} \tag{32}$$

By using expression (30), we have

$$\begin{aligned} \frac{\partial u}{\partial \vec{n}'}|_{K_A}(A) + \frac{\partial u}{\partial \vec{n}''}|_{L_A}(A) =& \alpha_1 \frac{\partial u}{\partial \overrightarrow{AK_A}}(A) + \alpha_2 \frac{\partial u}{\partial \overrightarrow{AL_A}}(A)\\ =& \alpha_1 \frac{uK_A - uA}{|K_A - A|} + \alpha_2 \frac{u(L_A)-u(A)}{|L_A - A|}\\ &+ O(h), \end{aligned} \tag{33}$$

and

$$\begin{aligned} \frac{\partial u}{\partial \vec{n}'}|_K(A) + \frac{\partial u}{\partial \vec{n}''}|_L(A) =& \beta_1 \frac{\partial u}{\partial \overrightarrow{KA}}(A) + \beta_2 \frac{\partial u}{\partial \overrightarrow{LA}}(A)\\ =& \beta_1 \frac{uA - uK}{|A-K|} + \beta_2 \frac{u(A)-u(L)}{|A-L|}\\ &+ O(h). \end{aligned} \tag{34}$$

Suppose that

$$\begin{aligned} &(\lambda(K_A) + \lambda(L_A))\left(\alpha_1 \frac{u_{K_A} - u_A}{|K_A - A|} + \alpha_2 \frac{u_{L_A} - u_A}{L_A - A}\right)\\ &= (\lambda(K) + \lambda(L))\left(\beta_1 \frac{u_A - u_K}{|A-K|} + \beta_2 \frac{u_A - u_L}{|A-L|}\right). \end{aligned} \tag{35}$$

We get

$$u_A = \frac{\zeta_1 u_{K_A} + \zeta_2 u_{L_A} + \zeta_3 u_K + \zeta_4 u_L}{\zeta_1 + \zeta_2 + \zeta_3 + \zeta_4} \tag{36}$$

where

$$\begin{aligned} \zeta_1 &= (\lambda(K_A) + \lambda(L_A))\frac{\alpha_1}{|K_A - A|}\\ \zeta_2 &= (\lambda(K_A) + \lambda(L_A))\frac{\alpha_2}{|L_A - A|}\\ \zeta_3 &= (\lambda(K) + \lambda(L))\frac{\beta_1}{|A-K|}\\ \zeta_4 &= (\lambda(K) + \lambda(L))\frac{\beta_2}{|A-L|} \end{aligned}$$

Let

$$\begin{aligned} \omega_{A_1} &= \frac{\zeta_1}{\zeta_1+\zeta_2+\zeta_3+\zeta_4},\\ \omega_{A_2} &= \frac{\zeta_2}{\zeta_1+\zeta_2+\zeta_3+\zeta_4},\\ \omega_{A_3} &= \frac{\zeta_3}{\zeta_1+\zeta_2+\zeta_3+\zeta_4},\\ \omega_{A_4} &= \frac{\zeta_4}{\zeta_1+\zeta_2+\zeta_3+\zeta_4}, \end{aligned} \tag{37}$$

Similarly, $\omega_{B_1}(i = 1, 2, 3, 4)$ can be defined.

From expression (36), we have

$$\begin{aligned} u_A &= \omega_{A_1} u_{K_A} + \omega_{A_2} u_K + \omega_{A_3} u_L + \omega_{A_4} u_{L_A},\\ u_B &= \omega_{B_1} u_K + \omega_{B_2} u_{K_B} + \omega_{B_3} u_{L_B} + \omega_{B_4} u_L. \end{aligned} \tag{38}$$

Open Science Index, Mathematical and Computational Sciences Vol:4, No:10, 2010 publications.waset.org/5135.pdf

It follows that

$$\mathbf{F}_{K,\sigma} = \begin{cases} -\tau_\sigma \left[u_L - u_K \right. \\ -D_\sigma \left(\omega_{A_1} u_{K_A} + \omega_{A_2} u_K + \omega_{A_3} u_L + \omega_{A_4} u_{L_A} \right. \\ \left. \left. - \left(\omega_{B_1} u_K + \omega_{B_2} u_{K_B} + \omega_{B_3} u_{L_B} + \omega_{B_4} u_L\right)\right)\right], \\ \forall \sigma \in \mathcal{E}_{int}^0, \\ \\ -\tau_\sigma \left[u_L - u_K \right. \\ \left. -D_\sigma \left(\omega_{A_1} u_{K_A} + \omega_{A_2} u_K + \omega_{A_3} u_L + \omega_{A_4} u_{L_A}\right)\right], \\ \forall \sigma \in \mathcal{E}_{int}, B \in \partial\Omega, \\ \\ -\tau_\sigma \left[u_L - u_K \right. \\ \left. +D_\sigma \left(\omega_{B_1} u_K + \omega_{B_2} u_{K_B} + \omega_{B_3} u_{L_B} + \omega_{B_4} u_L\right)\right], \\ \forall \sigma \in \mathcal{E}_{int}^0, A \in \partial\Omega, \\ \\ \tau_{K,\sigma} u_K, \forall \sigma \in \mathcal{E}_{ext}. \end{cases} \tag{39}$$

The stability and convergence of the resulting scheme are proved in [6] as well as the numerical results obtained on different meshes for several test problems to show the accuracy and the efficient of the method.

III. The Magnetic Field Equations and 2-D Solver

Figure 4 shows a cross section of the computational region defined for the model. All three-dimensional effects are omitted, and a cylindrically symmetric region is considered. A further approximation made is to neglect coil motion in the field solver. No field calculations take place in the conductors in axial regions below the point of contact, primarily because these regions are decoupled by the turns shorting and do not affect the generator performance.

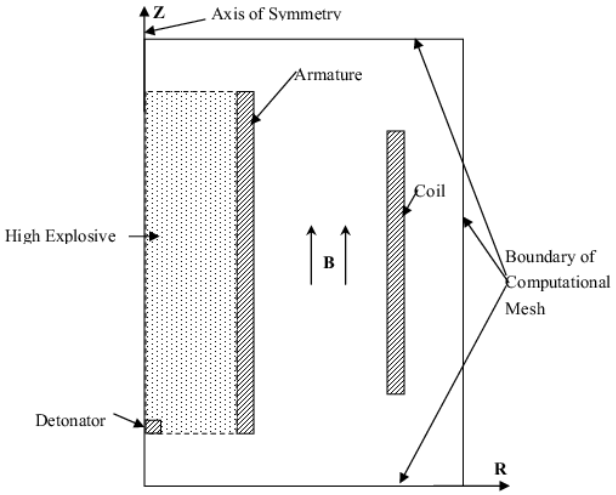

Fig. 4. Computational region.

In computing magnetic fields in cylindrical coordinates, it is often convenient to employ the magnetic stream function $\Psi = rA_\theta$, where A_θ is the azimuthal component of the vector potential. The use of the stream function insures that the divergence of the magnetic field is identically zero, and it is generally simpler to solve a single equation for Ψ (with $B_z = \frac{1}{r}\frac{\partial \Psi}{\partial r}$ and $B_r = -\frac{1}{r}\frac{\partial \Psi}{\partial z}$), rather than two equations for the components of the magnetic field.

The solution for the stream function requires boundary conditions at all boundaries of the active mesh. Guided by experimental results, we have assumed that no flux flows through either the inner armature boundary or the outer boundary of the coil, so that the stream function is held fixed at the initial value on those boundaries. Boundary conditions for the axial boundaries are less well-defined, but we have assumed that a condition of $\frac{\partial \Psi}{\partial z} = 0$ at the two ends is representative of the actual device.

To derive the stream function equations we combine Maxwell's equations

$$\nabla \times \vec{E} = -\frac{\partial \vec{B}}{\partial t} \tag{40}$$

$$\nabla \times \vec{B} = \mu_0 \vec{J} \tag{41}$$

where the displacement current has been dropped in Eq. (41), with Ohm's law

$$\vec{J} = \sigma \left[\vec{E} + \vec{v} \times \vec{B}\right], \tag{42}$$

where σ is the electrical conductivity. Using the definition $\nabla \times \vec{A} = \vec{B}$ and $\vec{E} = -\frac{\partial \vec{A}}{\partial t}$, one obtains the vector potential equation

$$\frac{\partial \vec{A}}{\partial t} = -\frac{1}{\mu_0 \sigma} \nabla \times (\nabla \times \vec{A}) + \vec{v} \times \nabla \times \vec{A}, \tag{43}$$

If we write this in cylindrical coordinates in terms of a single component $\Psi = rA_\theta$, the final result is

$$\frac{\partial \Psi}{\partial t} = \frac{1}{\mu_0 \sigma}\left(\frac{\partial^2 \Psi}{\partial r^2} + \frac{\partial^2 \Psi}{\partial z^2}\right) - \left(v_r + \frac{1}{\mu_0 \sigma r}\right)\frac{\partial \Psi}{\partial r} - v_z \frac{\partial \Psi}{\partial z}, \tag{44}$$

In the vacuum region, the current density is zero, so that one has

$$\frac{\partial^2 \Psi}{\partial r^2} - \frac{1}{r}\frac{\partial \Psi}{\partial r} + \frac{\partial^2 \Psi}{\partial z^2} = 0. \tag{45}$$

The basic sequence of operations in the coupled hydro/magnetic field calculation begins with initialization of all hydro and field quantities. The hydro variables are advanced one time step and are used to define the new conductor configurations and velocities. These new velocities are used with Eq. (44) to update the stream function in the conductor regions to the new level. After the conductor regions solution is updated, the updated vacuum solution is obtained from Eq. (45). This completes the time step and the process repeats, again beginning with the hydro variables. The fully self-consistent version of the code will compute magnetic forces and Joule heating contributions at the end of the field solver calculation to be used in the next advancement of the hydro variables.

Open Science Index, Mathematical and Computational Sciences Vol:4, No:10, 2010 publications.waset.org/5135.pdf

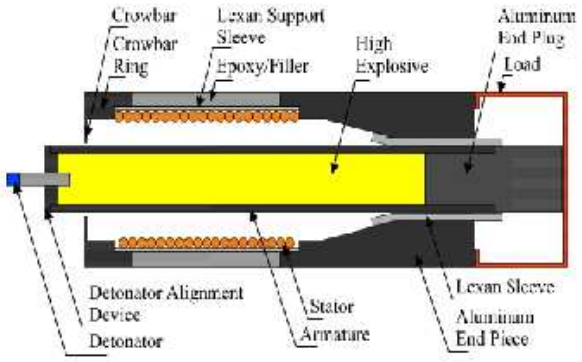

Fig. 5. Schemas of simple winded HMFCG.

TABLE I
PARAMETERS OF TTU-1(SERIES TTU1)

Diameter of coil core: 2mm	
Outer radius of coil	33mm
Inner radius of coil	31mm
Conductance of Cu	$5.8\times10^7(1/\Omega\cdot m)$
Pitch of coil	3mm
Width of armature: 3mm	
Outer radius of Al-armature	19.05mm
Inner radius of Al-armature	16.05mm
Conductance of Al	$3.6\times10^7(1/\Omega\cdot m)$
Turns	32

IV. NUMERICAL CALCULATION

In this section the results of APMFCG calculation are given. The basic parameters of MFCG are selected from a simply winded HMFCG in Texas Tech University [5] mainly.

Figures (6) compare the computed and experimental currents with two different seed current. It shows an acceptable agreement.

Figure (7) show the circuit characteristic of the device.

V. CONCLUSION

We have described the construction of a finite volume scheme for diffusion equations and a 2-D magnetic field solver designed specifically for the MFCG application.

There are many possible reason for the disagreement including turn-to-turn electrical breakdown in the coil, delayed electrical shorting of the armature and coil caused by the insulating material, instabilities or three-dimensional behavior in armature expansion, venting of explosive gases into the region between the armature and coil, residual inductances of the generator output and return connections, and three-dimensional effects at the end of the generator where the helical coil couples to the output connectors. These and other effects are under study.

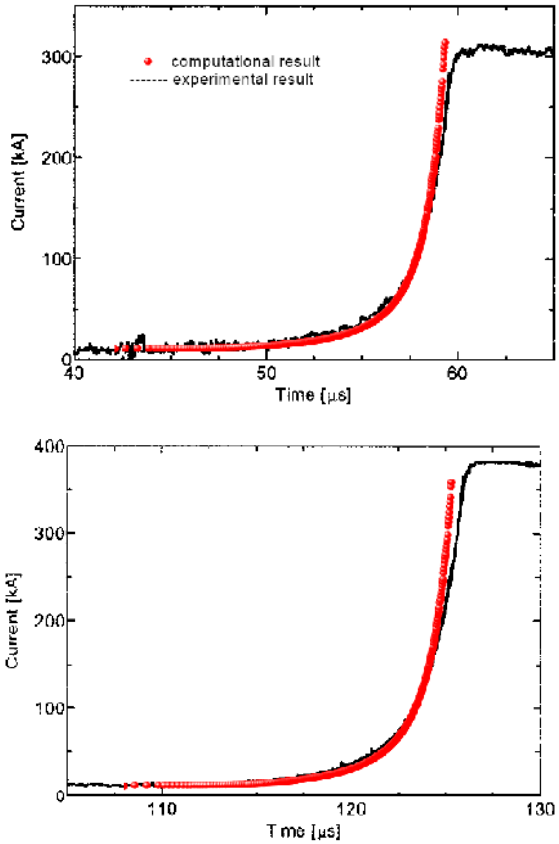

Fig. 6. (up)($I_0 = 8kA$); (bottom)($I_0 = 12kA$)

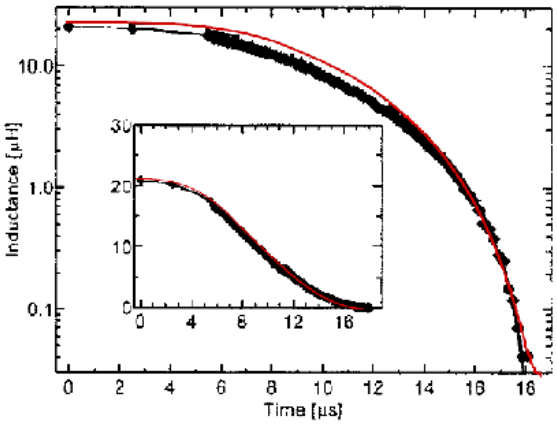

Fig. 7. Coil inductance for TTU-1.

REFERENCES

[1] H. Knoepfel, *Pulsed High Magnetic Fields*, North-Holland, Amsterdam, 1970.
[2] C. M. Fowler, Science, Vol.180, pp.261, 1973.
[3] J. W. Shear et al., J. Appl. Phys., Vol.39, pp.2102, 1968.
[4] J. C. Crawford and R. A. Damerow, J. Appl. Phys., Vol.39, pp.5224, 1968.
[5] J. Dickens and J. B. Comette and K. Jamison and E. R. Parkinson, *Electrical Behavior of a Simple Helical Flux Compression Generator for Code Benchmarking*, IEEE Transactions on Plasma Science, Vol.29, pp.4, 2001.
[6] Qiang Zhao and Guangwei Yuan, *Analysis and construction of cell-centered finite volume scheme for diffusion equations on distorted meshes*, Computer Methods in Applied Mechanics and Engineering, Vol.198,pp.3039-3050, 2009.